VSP

*Journal of Biomaterials Science 22 (2011) 1131–1146*

Journal of BIOMATERIALS SCIENCE
brill.nl/jbs

# Anti-tumor Activity of Biodegradable Polymer-Paclitaxel Conjugate Micelles on Lewis Lung Cancer Mice Models

**Yanhui Wan [a], Yonghui Zheng [b], Xiangfu Song [c], Xiuli Hu [b], Shi Liu [b], Ti Tong [a] and Xiabin Jing [b,*]**

[a] The First Hospital, Jilin University, Changchun 130021, P. R. China

[b] State Key Laboratory of Polymer Physics and Chemistry, Changchun Institute of Applied Chemistry, Chinese Academy of Sciences, Changchun 130022, P. R. China

[c] School of Public Health, Jilin University, Changchun 130021, P. R. China

Received 11 January 2010; accepted 30 March 2010

**Abstract**

Two kinds of paclitaxel (PTX) conjugate nanomicelles were prepared for cell apoptosis and anti-tumor activity evaluation on Lewis lung cancer mice models. One (PTX micelles) was prepared by self-assembling the PTX-conjugate co-polymer, poly(ethylene glycol)-b-poly(L-lactide-co-2-methyl-2-carboxyl-propylene carbonate/PTX), and the other (FA–PTX micelles) was by co-assembling a mixture of the folic acid (FA)-carrying co-polymer poly(ethylene glycol)-b-poly(L-lactide-co-2,2-dihydroxylmethyl-propylene carbonate/FA) (PEG-b-P(LA-co-DHP/FA)), and the PTX-conjugate co-polymer. At 7 and 14 days after tail intravenous injection, the mice were killed. The inhibition rates of tumor growth for PTX and FA–PTX micelles were 50 and 90%, respectively, on the day 7, and 33 and 71%, respectively, on the day 14 after drug injection. Flow cytometry analysis showed that the cell apoptosis rates were 43, 54 and 72% for the control group, PTX micelles group and FA–PTX micelles group, respectively, on the day 7, and 16, 25 and 42 on the day 14. With the TUNEL assay, the grey values of PTX micelles and FA–PTX micelles groups were determined to be 61–62% and 43–44%, of that of the control group, on day 7 or day 14, respectively. Therefore, the PTX micelles and the FA–PTX composite micelles significantly inhibited the subcutaneously inoculated Lewis lung cancer and effectively induced the cell apoptosis, and the FA–PTX composite micelles displayed a better efficacy than the PTX-micelles, implying the contribution of the folate-mediated targeting and endocytosis effect.



**Keywords**

Lewis lung cancer, polymer–drug conjugate, paclitaxel, folic acid, targeted drug delivery, cell apoptosis

* To whom correspondence should be addressed. E-mail: xbjing@ciac.jl.cn



DOI:10.1163/092050610X500570

## 1. Introduction

Lung cancer is one of the most common malignant tumors threatening human health and life. According to statistics, in some European countries, in the United States and in major cities of China, the incidence of lung cancer ranked first in males of various tumors in the past 50 years. And in recent years, the lung cancer incidence rate of females significantly increased [1].

Paclitaxel (PTX), a natural anti-cancer active substance isolated from the Taxus species, has a good therapeutic effect on lung cancer, breast cancer, cervical cancer and other malignant tumors [2]. It has been widely used in clinical treatments of these cancers [3]. However, because of its low water solubility and strong adverse reactions such as allergies, low blood pressure, etc., its clinical use has been greatly limited [4, 5]. Thus, how to increase its water solubility and reduce its toxic side-effects has long attracted much research attention.

Liposomes have been used for cancer drug delivery and proved effective. In recent decades, drug-encapsulated nano-micelles from amphiphilic block co-polymers have attracted considerable attention [6, 7], due to their obvious advantages over liposomes, such as mechanical strength and stability, effective protection of the drugs, low toxicity, prolonged circulation in the blood, enhanced permeation and retention in cancer beds, etc. [8, 9]. However, initial burst drug-release cannot be avoided for them. To overcome this limitation, polymer–drug conjugates, especially biodegradable amphiphilic block co-polymer–drug conjugates, have been developed [10–12]. In these conjugates, the drug molecules are chemically combined to the polymer ends or side-chains, so that their release based on physical diffusion is eliminated. They can self-assemble into nanoscale micelles in aqueous media and therefore, they can be administrated by intravenous injection easily. The medicated micelles are taken up by the cells *via* endocytosis and the drug molecules are released from the conjugates rapidly because of the acidic conditions and the acid hydrolyses in the lysosomes [13, 14]. Therefore, these medicated micelles show high *in vitro* cytotoxicity to many cancer cells [15] and *in vivo* anti-cancer activity [16, 17].

An ideal drug can selectively destroy diseased cells but is not harmful to healthy cells. Based on the specific interactions discovered in biology, several antibodies or ligands have been attached to drug molecules, liposomes, or polymer micelles to achieve active targeting effect to the corresponding antigen- or receptor-overexpressing organs, tissues, or cells [15, 18–21].

As an active targeting moiety, folic acid (FA) or folate has been intensively studied for its unique advantages over other ligands or antibodies: (1) it does not exhibit immunogenicity as many proteins do; (2) its interaction with its receptors is specific and its receptors are only over-expressed in human tumor cells [20, 22, 23] such as ovarian cancer, endometrial cancer, lung cancer, kidney cancer, breast cancer, colon cancer and nasopharyngeal cancer cells, but not in normal tissues; therefore, real cancer cell targeting can be achieved; (3) owing to its simple structure and small size, its interference with the drug's pharmacokinetics is negligible; (4) its

cost is very low because its synthesis and purification is quite simple; (5) its carboxyl group is easy to react with OH or $NH_2$, and the reaction products retain its intrinsic activity. Therefore, it has been conjugated to several drug molecules, liposomes or polymersomes. Recently, it was attached to a tri-block co-polymer methoxy-poly(ethylene glycol)-b-poly(L-lactide)-b-poly(L-lysine) (PEG-b-PLA-b-PLL) *via* the reaction of its COOH with the pendant $NH_2$ groups on PLL block [24–27], preferred endocytosis in HeLa cells and enrichment in H22 tumor beds were observed for the folate-conjugated micelles [27]. However, folate-targeting biodegradable amphiphilic block co-polymer–drug conjugate micelles have been rarely reported up to now, let alone studies of such micelles in animal models.

In this paper, therefore, FA was chosen as the targeting moiety, but it was attached to a carrier polymer *via* an ester linkage instead of an amide linkage as in Ref. [27]. A real anti-cancer drug, PTX, is used instead of a model drug. Based on our previous work [28–30], the PTX is conjugated to another carrier polymer. These two carrier polymers have similar structures, and therefore, the both conjugates are co-assembled into composite micelles. These micelles are expected to have multiple functions, including water solubility, prolonged circulation, biodegradability, folate-receptor targeting and rapid cell uptake. Lewis lung tumor models were used to examine the tumor inhibition rate and cell apoptosis effect of the composite micelles.

## 2. Materials and Methods

### *2.1. Paclitaxel*

Paclitaxel for injection used in experiments was purchased from Wellso Pharmaceutical (certificate No. H109880066). Each ampoule contains 30 mg paclitaxel in 5 ml polyoxyethylene-castor oil (Cremophor)/ethanol (1:1) solution. Before injection, it was diluted to the desired ratios with normal saline purchased from Cornel Pharmaceutical. The PTX raw material (purity 99.5%) was purchased from Chongqing United Pharmaceutical. It was used for conjugation with polymer carrier without further purification.

### *2.2. Preparation of PTX Micelles*

Two carrier polymers were synthesized in our own laboratory according to the reported procedures [28, 31, 32]. They were amphiphilic di-block co-polymers MPEG-b-P(LA-co-MCC) and MPEG-b-P(LA-co-DHP). Both of them contained identical MPEG blocks of 5.0 kDa in molecular mass. MCC and DHP stand for trimethylene carbonate units with pendant carboxyl (COOH) and dihydroxyl (OH) groups, respectively. The total molecular masses of them were about 7.5 kDa, as determined by $^1$H-NMR.

Using the active COOH and OH groups on the carrier polymers, PTX and folic acid (FA, purchased from Beijing Aoboxing Universeen Bio-tech) were chemically attached to the carrier polymer to form the PTX–polymer conjugate (in short, PTX-conjugate) MPEG-b-P(LA-co-MCC/PTX) (1) and FA–polymer conjugate (FA-conjugate) MPEG-b-P (LA-co-DHP/FA) (2), respectively:

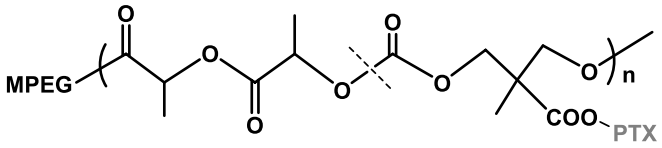


(1)

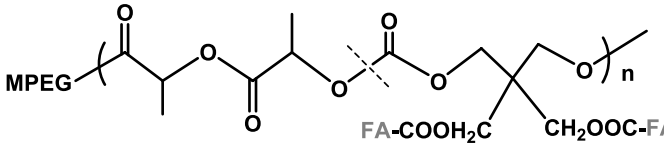


(2)

The PTX content in PTX-conjugate was 8 wt% as determined by high-pressure liquid chromatography, and the critical micelle concentration (CMC) of the PTX-conjugate was $2.5 \times 10^{-3}$ g/l measured by the pyrene fluorescence probe method [32].

Because of the amphiphilic nature of the PTX-conjugate (the MPEG segment was hydrophilic and P(LA-co-MCC/PTX) segment was hydrophobic), it was made into nanomicelles using a solvent replacement method (dissolving in THF, adding double-distilled water, rotary evaporation of THF), and then lyophilized to obtain freeze-dried powders of PTX–polymer conjugate micelles [30], hereinafter referred to as paclitaxel micelles or PTX micelles for short. Dynamic light scattering and transmission electron microscopy observation showed that the micelles had a spherical shape and had an average diameter of about 44 nm.

As shown in formula (2), the FA conjugate MPEG-b-P(LA-co-DHP/FA) was similar to the PTX-conjugate MPEG-b-P(LA-co-MCC/PTX) in di-block backbones, amphiphilic nature and comparable block lengths. The only difference between the two was that the carrier polymers were conjugated with PTX and FA, respectively. The folic acid content was measured by absorption spectroscopy (DMSO solution, 288 nm) to be 14 wt%. Therefore, the FA-conjugate was co-assembled with the PTX-conjugate in aqueous media by the following procedure: 90 mg PTX-conjugate and 10 mg FA-conjugate were dissolved in 10 ml DMF. The solution was added to a dialysis bag with $M_n$ cutoff = 3500 and was dialyzed against 1000 ml of double-distilled water for 24 h. The dialysis medium was replaced with fresh one every 4 h. After completion of dialysis, the solution was filtered through a 0.45-μm Millipore filter and was lyophilized. The freeze-dried powders were kept in a desiccator at 4°C in the dark.

The composite micelles obtained had a spherical shape and an average diameter of about 58 nm, identified by dynamic light scattering and transmission electron

microscopy. The critical micelle concentration (CMC) was $4.0 \times 10^{-3}$ g/l, as measured by pyrene fluorescence. The PTX content was 7.2 wt% and the FA content was 1.4 wt%. These micelles are referred to as FA–PTX composite micelles or FA–PTX micelles hereafter.

### 2.3. Cell Culture

The mouse Lewis lung cancer cell lines were purchased from Shanghai Cell Center of Chinese Academy of Medical Science. They were cultured in a glucose-enriched DMEM containing 10% fetal bovine serum, 100 units/ml penicillin and 100 μg/ml streptomycin, in a humidified incubator (Sanyo, Japan) containing 5% $CO_2$ at 37°C. The cells were harvested at their logarithmic phase of growth to ensure their regular shape and high reproductive ability. The cells were digested with 0.25% trypsin solution prepared with D-Hanks solution. Subculture was performed every 36 h. Finally, the cells were harvested, centrifuged at 800 rpm for 3 min, and re-suspended in 0.9% saline. The cell density was adjusted to $10^7$ cells/ml.

### 2.4. Lewis Lung Cancer Mice Models

C57BL/6 female mice, weighing 21–25 g, 50–60 days old, were purchased from the Institute of Laboratory Animals, Chinese Academy of Medical Science. They were adaptively raised for 7 days in an SPF level animal room. During the experiments, the mice in each group were allowed to drink running water and take rodent food freely and equally in an observational room at a temperature of 20–24°C and a relative humidity of 70–80%.

Sixty female C57BL/6 mice were subcutaneously injected with 0.1 ml Lewis lung cancer cells suspension (containing $1 \times 10^6$ living cells) each in the right hind limb. Eight days after the treatment, tumor nodules were observed visually in 53 mice and the diameters of the nodules as well as body weights were measured daily. On the 12th day, 40 tumor-bearing mice in good conditions (without hydrothorax or ascite, weighing $22.1 \pm 2.1$ g), with a diameter of the locally isolated tumor of 5.5–6.5 mm were selected and randomly divided into four groups, A, B, C and D (10 mice each). They were control group, commercial PTX (Taxol) group, PTX micelles group and FA–PTX micelles group, respectively. Of them, groups B–D were collectively referred to as drug groups.

The total drug amount for each mouse in drug groups was 20 mg/kg PTX, which was injected *via* the tail vein in three times as solutions in 0.9% saline, 0.5 ml each time, one time a day. Group A animals were injected with 0.5 ml of 0.9% saline each time. Seven and 14 days after drug administration, 5 mice in each group were killed to carry out related detections.

### 2.5. Tissue Treatment

The subcutaneous tumors in the right hind limb were carefully excised along the tumor capsule, washed with double distilled water, dried with filter paper and weighed. The tumor weights in one group were averaged to obtain the mean value

and standard deviation. The tumor inhibition rate (TIR) of each group was calculated by the equation: TIR = (1 − (mean tumor weight of test group/mean tumor weight of control group)) × 100%. Then the fresh tumor was divided equally into two parts. One part was used for flow cytometry and the other part was fixed with 10% paraformaldehyde solution, followed by immunohistochemistry and hematoxylin–eosin (HE) histological assays.

### 2.6. Detection and Quantification of Cell Apoptosis by TUNEL Assay

The fresh tumor tissue fixed with 10% para-formaldehyde solution for 48 h was embedded in paraffin wax and sectioned for TUNEL assay (Terminal deoxynucleotidyl transferase (TdT)-mediated deoxyuridine triphosphate (dUTP) nick end labeling). The TUNEL kit was purchased from Roche Diagnostics. It consisted of TdT from calf thymus (EC 2.7.7.31), dUTP labeled with digoxigenin (Dig-11-dUTP), and an anti-digoxigenin antibody conjugated with horseradish peroxidase (Fab-HRP). Briefly, the assay was carried out by following the kit instructions: (1) the tumor sections were dewaxed and dehydrated with xylene and ethanol, and permeabilized with a mixture of 0.1% Triton X-100 and 0.1% sodium citrate; (2) the TUNEL reaction was performed by adding a mixture solution of TdT and Dig-11-dUTP onto the tumor sections and incubating the sections in a humidified atmosphere in the dark at 37°C for 60 min; (3) the tumor sections were incubated with Fab-HRP solution for 30 min; (4) the tumor sections were stained with DAB (3,3′-diaminobenzidine tetrahydrochloride)/$H_2O_2$ mixture and incubated for 15 min; (5) the tumor sections were examined under a light microscope to measure the grey values (grey value is a measure of light brightness, expressed as a number from 0 (“black”) to 255 (“white”)). The grey values at the five different locations (central, upper, bottom, left and right zone) in the 400× micrograph of the section were read and averaged as the mean grey value of the section using the Motic Image Advanced 3.2 image analysis system (Jed Pella). The data of five such sections randomly obtained from one tumor tissue was averaged as the mean value of this mouse.

### 2.7. Flow Cytometry

The flow cytometer (BD FACSCalibur) was purchased from Becton Dickinson. The Annexin V-FITC/PI Apoptosis Detection kit was purchased from Yan-Bin Chemical Technology.

The flow cytometric analysis in the present study is based on the following principle: phosphatidylserine (PS) is normally located on the inner side of cell membrane for a live cell. In the early stage of apoptosis, PS flips from the inner side to the outer membrane surface and, thus, is exposed to the extracellular environment. Annexin V is a $Ca^{2+}$-dependent phospholipid-binding protein with a high affinity for PS. Therefore, Annexin V labeled by FITC (fluorescein isothiocyanate) as a fluorescence probe can be used to detect the occurrence of apoptosis. Propidium iodide (PI) is a nucleic dye which can not penetrate the normal cell membrane, but it can make the nucleus of late apoptotic cells or dead cells be dyed red so as to distin-

guish them from normal cells or early apoptotic cells. Therefore, by double staining with Annexin V-FITC and PI, cell apoptosis can be detected.

The analysis was performed on a cell suspension prepared from the cancer tissue. The tumor cell suspension was prepared by consecutively cutting the fresh tumor tissue into small pieces in cold PBS (pH 7.2–7.4, 0–4°C) and grinding the small pieces between microscope slides, then filtering the mixture with a 200-mesh filter. The filtrate was centrifuged at 500 rpm for 5 min (Sorvall Biofuge Stratos) to remove the cell debris in the supernatant and the isolated sediment was washed twice with cold PBS, and finally re-suspended in cold PBS. After adjusting the cell density with the help of a hemocytometer, the cell suspension that contained at least $1 \times 10^6$ cells was incubated with Annexin V-FITC and PI for 30 min, and then analyzed on the flow cytometer, using the untreated cells as negative control and the standard Annexin V-FITC and dissolved PI single-stained tubes for fluorescence calibration.

The data from the Cellquest software (Becton Dickinson) were analyzed with ModFit software (Verity Software House), and were expressed in two-parameter histograms with Annexin V-FITC count on the $x$-axis and PI count on the $y$-axis. Therefore, the four quadrants could be assigned to normal cells (LL, Annexin−/PI−), necrotic cells (UL, Annexin−/PI+), early apoptotic cells (LR, Annexin+/PI−) and late apoptotic cells (UR, Annexin+/PI+), respectively. The total cell apoptosis rate was (UR + LR).

### *2.8. Hematoxylin–Eosin (HE) Staining*

The tumor tissue fixed for 48 h in 10% para-formaldehyde solution was dehydrated, embedded in rosin, sectioned and stained with a HE staining kit (Sigma-Aldrich). The morphology of the cells was observed under an optical microscope. The violet pots stand for the nuclei and the red areas stand for the cell plasma.

### *2.9. Statistical Analysis*

The results were analyzed using statistical software PSS13.0, each set of data was given as mean ± SD. Difference comparison between groups was carried out by single factor variance analysis. $P < 0.05$ is considered as significant.

## 3. Results

### *3.1. General Status Observation*

The Taxol group mice were dysphoric and screamed from time to time during drug injection. They exhibited cachexia, reduction of hair-luster, reduction of appetite and other adverse reactions in the first 2 days after drug injection, and they recovered from these reactions gradually 3 days thereafter. Mice of other groups had no obvious adverse reactions. One mouse in the FA–PTX micelle group died when it was injected for the third time.

### 3.2. Tumor Growth Inhibition

The photographs of the excised tumors of all groups 7 and 14 days after the drug administration are shown in Fig. 1. Their weights are collected in Table 1. Based on these data, TIR values were calculated.

As shown in Table 1, the three drug groups displayed an obvious tumor-inhibition effect. On day 7 after drug administration, they had a very significant difference ($P < 0.01$) in tumor weight compared with the control group, while the anti-tumor effect of FA–PTX micelles group was superior to Taxol and PTX micelles groups ($P < 0.05$). On day 14, there was still a statistically significant difference ($P < 0.05$) between the drug groups and the control group, and between the FA–PTX micelle group and the Taxol or the PTX micelles group.

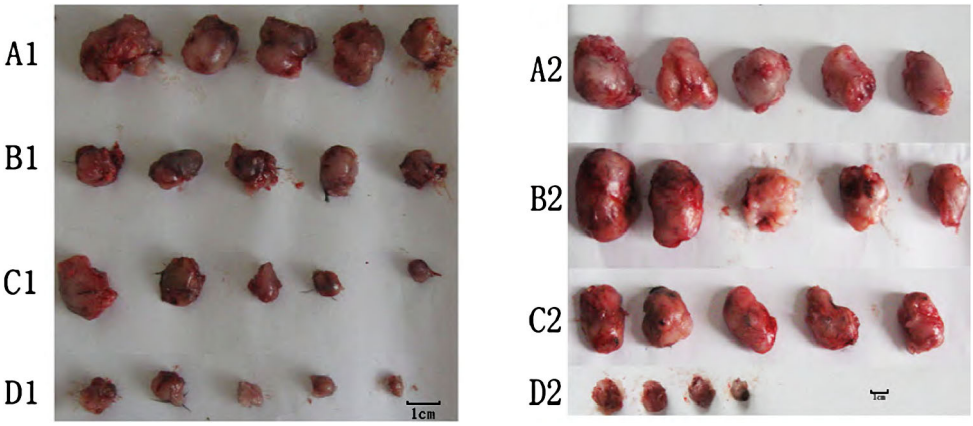


**Figure 1.** Tumor tissues from the mice models. (A) Control group, (B) Taxol group, (C) PTX micelles group and (D) FA–PTX micelles group. (A1–D1) On day 7 after drug administration, (A2–D2) on day 14 after drug administration. Scale bars = 1 cm. This figure is published in colour in the online edition of this journal, that can be accessed *via* http://www.brill.nl/jbs

**Table 1.**
Tumor weights and tumor inhibition rates (TIR) data (mean ± SD)

| Group | Day 7 | | | Day 14 | | |
|---|---|---|---|---|---|---|
| | *n* | *W* (g) | TIR (%) | *n* | *W* (g) | TIR (%) |
| Control | 5 | 2.64 ± 1.06** | – | 5 | 4.74 ± 1.46** | – |
| Taxol | 5 | 1.25 ± 0.18*,** | 52.6 | 5 | 3.21 ± 1.55** | 32.2 |
| PTX micelles | 5 | 1.31 ± 0.66*,** | 50.3 | 5 | 3.17 ± 0.46** | 33.0 |
| FA–PTX micelles | 5 | 0.27 ± 0.14* | 89.7 | 4 | 1.37 ± 0.79 | 71.3 |

*$P < 0.05$, compared with control group; **$P < 0.05$, compared with FA–PTX micelles group; *n*, number of mice in one group; *W*, tumor weight; TIR, tumor inhibition rate.

### 3.3. Apoptosis Detection of Tumor Cells by TUNEL Assay

As shown in Table 2 and Fig. 2, the TUNEL assay revealed statistically significant differences between the drug groups and the control group ($P < 0.01$) and between the FA–PTX micelles group and the other two drug groups ($P < 0.01$), either on day 7 or on day 14 after drug administration. The grey values followed the order control > Taxol > PTX micelles > FA–PTX micelles.

### 3.4. Flow Cytometry Assay

The apoptosis rates of the tumor cells were evaluated by flow cytometry using Annexin V-FITC and PI double staining. All the Annexin-V-positive cells were considered as apoptotic ones. As shown in Fig. 3 and Table 3, the apoptosis rates of the control group were significantly lower than those of the drug groups on days 7 and 14 after drug administration ($P < 0.05$), and there were also significant differences in apoptosis rate between the FA–PTX micelles group and the other two drug

**Table 2.**
Grey values measured by TUNEL assay (mean ± SD)

| Group | Day 7 | | Day 14 | |
|---|---|---|---|---|
| | *n* | Grey value | *n* | Grey value |
| Control | 5 | 235 ± 3.0 | 5 | 235 ± 3.4 |
| Taxol | 5 | 183 ± 3.2 | 5 | 182 ± 3.6 |
| PTX micelles | 5 | 145 ± 1.1 | 5 | 144 ± 3.6 |
| FA–PTX micelles | 5 | 100 ± 1.6 | 4 | 102 ± 6.4 |

All differences between any two groups are very significant ($P < 0.01$); *n*, number of mice in one group.

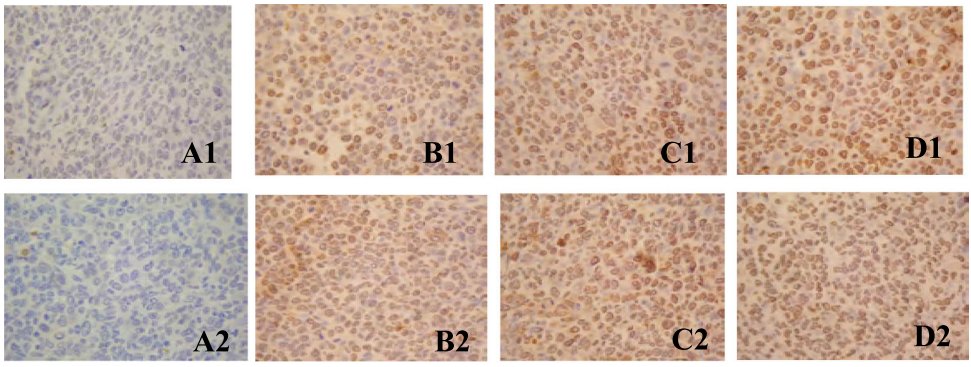


**Figure 2.** Apoptosis detection of the tumor cells by TUNEL assay (400×). (A) Control group, (B) Taxol group, (C) PTX micelles group and (D) FA–PTX micelles group. (A1–D1) On day 7 after drug administration, (A2–D2) on day 14 after drug administration. This figure is published in colour in the online edition of this journal, that can be accessed *via* http://www.brill.nl/jbs

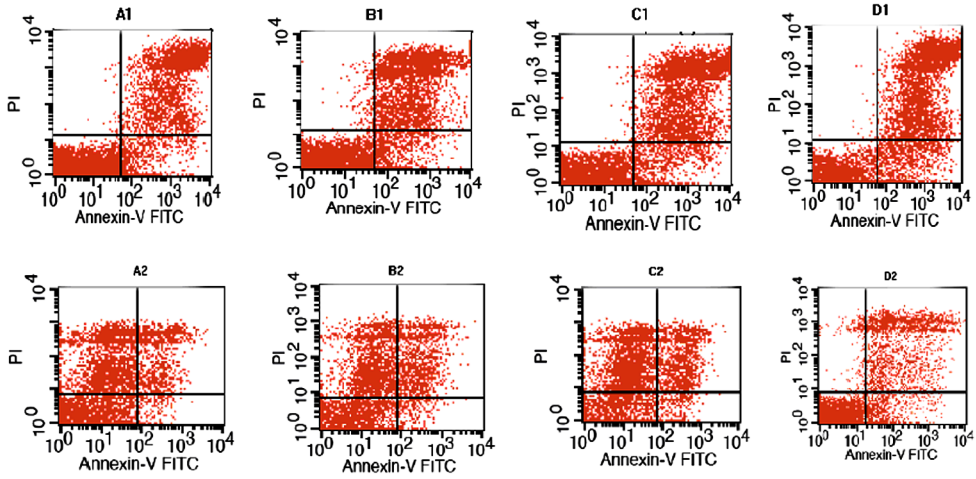


**Figure 3.** Flow cytometry results of the tumor cells. (A) Control group, (B) Taxol group, (C) PTX micelles group and (D) FA–PTX micelles group. (A1–D1) On day 7 after drug administration, (A2–D2) on day 14 after drug administration. This figure is published in colour in the online edition of this journal, that can be accessed *via* http://www.brill.nl/jbs

**Table 3.**
Apoptosis rates of the tumor cells determined by flow cytometry (mean ± SD)

| Group | Day 7 | | Day 14 | |
|---|---|---|---|---|
| | *n* | CAR (%) | *n* | CAR (%) |
| Control | 5 | 42.9 ± 2.1** | 5 | 16.3 ± 2.4** |
| Taxol | 5 | 52.0 ± 1.7*,** | 5 | 25.3 ± 4.2*,** |
| PTX micelles | 5 | 53.8 ± 2.1*,** | 5 | 24.1 ± 3.3*,** |
| FA–PTX micelles | 5 | 72.1 ± 0.8* | 4 | 42.4 ± 3.8* |

* $P < 0.05$, compared with control group; ** $P < 0.05$, compared with FA–PTX micelles group; *n*, number of mice in one group; CAR, cell apoptosis rate.

groups ($P < 0.05$). Moreover, on day 7 after drug administration, the percentage of apoptosis was in the order control < Taxol < PTX micelles < FA–PTX micelles, while on day 14 the order was control < Taxol ≈ PTX micelles < FA–PTX micelles.

### *3.5. Histopathological Examination*

Typical pathological photographs (HE staining) are shown in Fig. 4. It is seen that the tumor cells in the control group retained the heteromorphism as in the original cultured state, such as irregular shape, enlarged and darker stained nuclei and nuclearatypia. The fibrosis of tumor cells, tissue hemorrhage and necrosis were seen in

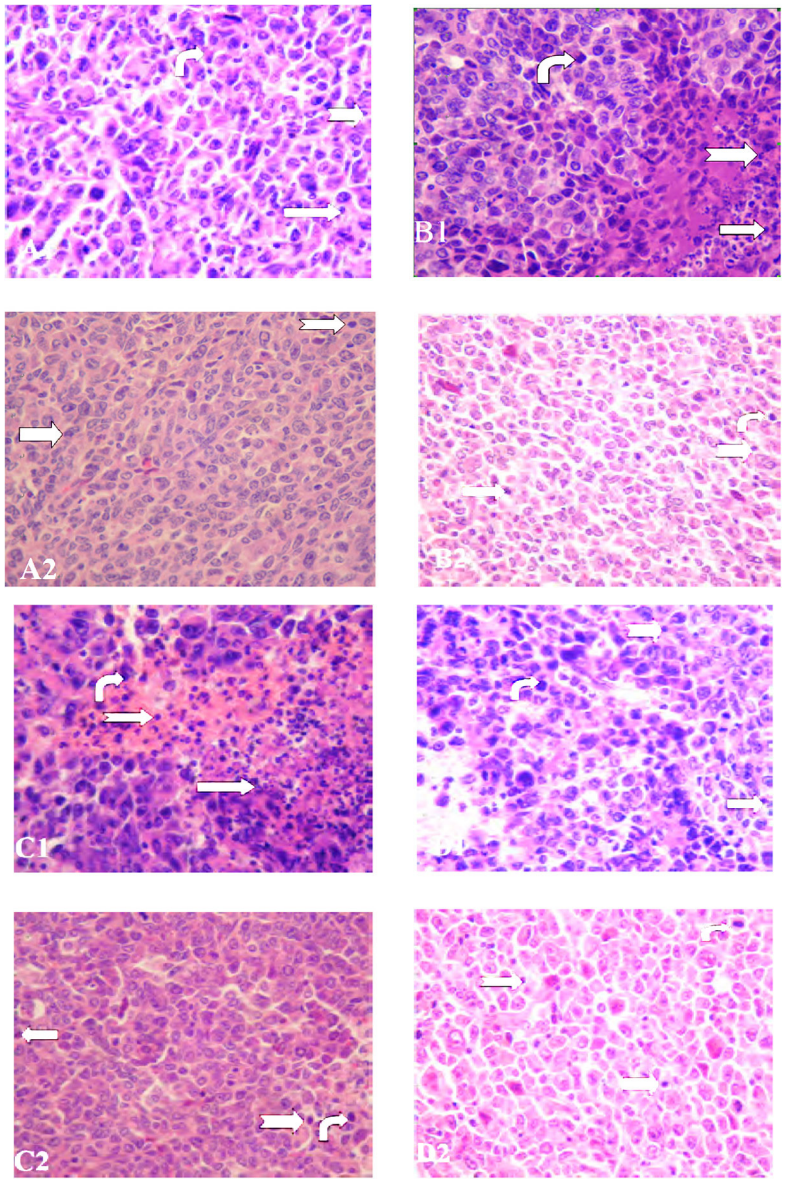


**Figure 4.** Histopathological micrographs (HE staining, 400×) of the tumor slices. (A) Control group, (B) Taxol group, (C) PTX micelles group and (D) FA–PTX micelles group. (A1–D1) On day 7 after drug administration, (A2–D2) on day 14 after drug administration. Special cells: macrophages (curved arrows), neutrophils (straight arrows) and lymphocytes (swallowtail arrows). This figure is published in colour in the online edition of this journal, that can be accessed *via* http://www.brill.nl/jbs

the three drug groups, and the degree of cell fibrosis and the areas of tissue hemorrhage and necrosis significantly increased in the order Taxol group < PTX micelles group < FA–PTX micelles group.

Further examination showed that there existed a few macrophages, neutrophils and lymphocytes in the tumor tissue section. The macrophages (indicated in Fig. 4 by the curved arrows) appeared within the necrotic area of the section at a density of 0–2 per field of vision of 400× and they were surrounded by apoptosis cells with shrunk shapes as an indication of phagocytosis and clearance reaction after cell apoptosis. The neutrophils (indicated by the straight arrows) and lymphocytes (indicated by the swallowtail arrows) were surrounding the necrotic area with a density of 1–4 per field of vision of 400×, as an indication of inflammatory response to the tumor cells.

## 4. Discussion

Disruption of tumor cell apoptosis is an important mechanism for tumorgenesis. Formation of malignant tumors is the direct result of the loss of spontaneous apoptosis of cells. Therefore, to induce apoptosis of tumor cells is the main objective and means of cancer therapy. It is even more desirable than to inhibit tumor cell proliferation [33]. The function of PTX is to promote tubulin polymerization and to stabilize the microtubules and, in turn, to break the balance between polymerization and depolymerization of tubulins, thereby preventing the growth of cancer cells and causing apoptosis [34]. In the present study, PTX is used as anti-tumor agent. It is well known and widely accepted by doctors and patients. It is conjugated to an amphiphilic block co-polymer, MPEG-b-P(LA-co-MCC). Both the carrier polymer and the PTX-conjugate are amphiphilic and can self-assemble into nanoscale micelles with PTX in the core of the micelles and the PEG in the corona of the micelles. Therefore, PTX is highly solubilized and effectively protected. The PTX micelles are water soluble and can be injected as normal water-based formulations without the use of polyoxyethylene castor-oil/ethanol solvent. Therefore, the reverse side-effects associated with castor-oil are avoided, and the animals of the PTX micelles group and FA–PTX composite micelles group do not show appreciable allergic reactions as the Taxol group animals do.

In order to realize active targeting to the cancer bed, FA is introduced to the micelles, because it is well known that FA-receptors are over-expressed by many malignant carcinoma cells. By means of the specific interaction between FA and FA-receptors, cancer cell targeting can be achieved and endocytosis can be enhanced. In the present study, FA is neither attached to the PTX molecule, nor to the macromolecule that carries the PTX, but to another block co-polymer, MPEG-b-P(LA-co-DHP), which has identical block structure to the PTX carrier polymer. For this reason, the FA-conjugate MPEG-b-P(LA-co-DHP/FA) may co-assemble with the PTX-conjugate to form FA–PTX composite micelles, in which the PTX content is 7.2 wt% and the FA content is 1.4 wt%. As shown in this study, incorporation of FA moiety significantly enhances the anti-cancer efficacy of PTX.

In all animals examined, the tumors keep growing, but the growth rates are different from group to group. Compared to the control group, three drug groups exhibit

obvious cancer size and weight suppression. The inhibition rates of Taxol, PTX micelles and FA–PTX micelles groups on day 7 after administration are 52, 50 and 90%, respectively, a very significant difference ($P < 0.01$) from the control group. Among the three drug groups, the FA–PTX micelles group is statistically significantly different from the other two (Taxol, PTX micelles) ($P < 0.05$). The inhibition rates of the drug groups on day 14 day after administration are 32, 33 and 71%, respectively. Their absolute values are smaller than the corresponding data on day 7, probably due to the limited amounts of PTX available in the animal bodies. Because of continuous release and consumption, the effective dose of PTX decreases to such a level after 7 days that the PTX available can not suppress cancer growth any longer. It suggests that PTX micelles or FA–PTX micelles should be administered in proper frequency to maintain the minimum concentration. Nevertheless, the differences from the control group are obvious. The difference between the FA–PTX micelles group and control group is significant ($P < 0.05$) while the $P$ values between the Taxol and PTX micelles groups and the control group are 0.059 and 0.054, respectively. Although they do not meet the significance standard, they are still very close to it. Moreover, the inhibition rate of FA–PTX micelles group is 71%, significantly different from the other two drug groups ($P < 0.05$). These results suggest that the PTX nanomicelles and FA–PTX nano-micelles can effectively suppress the growth of Lewis lung cancers. Among them, the inhibition rate of PTX nanomicelles is about 52% on day 7 and 32% on day 14 after drug administration, comparable to that of commercial Taxol. The inhibition rate of FA–PTX composite micelles reaches 90% on day 7 and 71% on day 14, making significant differences from Taxol or single PTX micelles. This improvement is ascribed to the incorporation of FA moieties. The folic acid receptor mediated targeting and endocytosis brings about enhanced anti-cancer efficacy of the composite micelles.

In the present study, cell apoptosis is assessed by both flow cytometry and TUNEL assay. As shown in Table 3, cell apoptosis rates on day 7 after administration are 43% for the control group, 52–54% for the Taxol and PTX micelles groups, and 72% for FA–PTX micelles group, with a significant statistical difference among the three ($P < 0.05$). These rates on day 14 after administration are decreased compared with day 7 data, in agreement with the tumor weight measurement, but a difference between groups can still be seen: from 16% for the control group, to 24–25% for the Taxol and PTX micelles groups, and then to 42% for the FA–PTX micelles group, with a significant difference between the three ($P < 0.05$). This shows that Taxol, PTX micelles and FA–PTX micelles can induce cell apoptosis in the Lewis lung cancer cells. Of them, FA–PTX micelles are more effective. This is consistent with the results of the tumor weight measurement. It should be particularly pointed out here that although the operations of cell preparation and treatment are exactly the same on day 7 and on day 14, the two-parameter histograms of the flow cytometry (Fig. 3) are different: much more data points appear in the UL quadrant for day 14 than for day 7. It means that much more necrotic cells are detected in the day 14 samples. The cancerous cells become so weak that they cannot afford

the grinding. Many of them are destroyed during the cell preparation. This may be one of the reasons for the low apoptosis rates on day 14. Taking this part of dead cells into consideration, the corrected apoptosis rates would be higher. On the other hand, of the four groups, the FA–PTX micelles group gives much less population in the UL quadrant. It implies that the cells of this group are strong enough to survive the sample preparation. In this sense, FA–PTX micelles are more efficient to suppress the cancer growth.

The TUNEL assay is usually sensitive to cell apoptosis [35, 36]. The evaluation is performed on the fixed cancer sections, not on individual cells and, therefore, no cell damage is involved as in the case of flow cytometry. As shown in Fig. 2 and Table 2, the four groups display statistically very different grey values either on day 7 or on day 14. Taking the grey value of the control group as unity, those of the three drug groups are 78, 62 and 43%, respectively, on day 7, and 77, 61 and 44%, respectively, on day 14. These two sets of data are correspondingly identical, indicating the similarity between the day 7 samples and the day 14 samples. This supports our previous analysis on the flow cytometric results.

The histopathological assay by HE staining shows that the tumor cells change their morphology and characteristics after drug treatment; for example, formation of fibrosis, tissue hemorrhage and necrosis, and the degree of cell fibrosis and the areas of tissue hemorrhage and necrosis significantly increase in the order Taxol group $<$ PTX micelles group $<$ FA–PTX micelles group. This is in agreement with the above flow cytometry and TUNEL observations. Because the carrier polymers in the micelles, MPEG-b-P(LA-co-MCC) and MPEG-b-P(LA-co-DHP), are both non-immunogenic, the related immunological responses were not observed. Instead, a few neutrophils, lymphocytes and macrophages are found around and within the necrotic area of the tumor tissue section, respectively, indicative of inflammatory response to the tumor cells, and phagocytosis and clearance reaction after cell apoptosis.

In conclusion, PTX-conjugate micelles and both FA and PTX-conjugate composite micelles of spherical shape and of 40–60 nm diameter have been successfully prepared by self-assembling or co-assembling related amphiphilic block copolymers. In these micelles, PTX content is 7–8%. It is wrapped in the core part of the micelles. The hydrophilic PEG segments constitute the corona of the micelles, leading to effective solubilization of the PTX and protection of the micelle system against the immunological system. Therefore, they can be administered *via* tail vein injection into Lewis lung tumor-bearing mice smoothly. At the dose of 20 mg/kg, the PTX micelles and FA–PTX micelles exhibit significant anti-tumor effects. The tumor inhibition rates are 50 and 90% on day 7 after administration, and remain 33 and 71% on day 14 after administration. The apoptosis rates detected by flow cytometry of the two micelle groups are 1.25 times and 1.68 times of that of the control group, respectively, on day 7 and 1.51 times and 2.63 times, respectively, on day 14. The grey values of the two micelle groups detected from tissue biopsy photos by the TUNEL method are 62 and 43% on day 7 compared with that of the control

group, and 61 and 44% on day 14. These data indicate that PTX-conjugate micelles and FA–PTX composite micelles have significant tumor inhibition and apoptosis induction effect on the subcutaneous Lewis lung tumors in mice models, and the FA–PTX composite micelles exhibit more efficacy than PTX micelles because of the FA-receptor-mediated tumor targeting and endocytosis of the micelles.

*Acknowledgements*

Financial support was provided by the National Natural Science Foundation of China (Project No. 20674084, 50733003, A3 Foresight Program No. 2062114 0369), and by the Ministry of Science and Technology of China ("973 Project" No. 2009CB930102 and "863 Project" No. 2007AA03Z535).

## References

1. H. Jiang, *Jpn. J. Clin. Oncol.* **39**, 137 (2009).
2. P. Crosasso, M. Ceruti, P. Brusa, S. Arpicco, F. Dosio and L. Cattel, *J. Control. Rel.* **63**, 19 (2000).
3. J.-q. Kong, W. Wang, P. Zhu and K.-d. Cheng, *Yaoxue Xuebao* **42**, 358 (2007).
4. E. K. Rowinsky and R. C. Donehower, *New Engl. J. Med.* **332**, 1004 (1995).
5. R. B. Weiss, R. C. Donehower, P. H. Wiernik, T. Ohnuma, R. J. Gralla, D. L. Trump, J. R. Baker, D. A. Vanecho, D. D. Vonhoff and B. Leyland-Jones, *J. Clin. Oncol.* **8**, 1263 (1990).
6. S. A. Jenekhe and X. L. Chen, *Science* **279**, 1903 (1998).
7. A. Rosler, G. W. M. Vandermeulen and H. A. Klok, *Adv. Drug Deliv. Rev.* **53**, 95 (2001).
8. M. L. Adams, A. Lavasanifar and G. S. Kwon, *J. Pharm. Sci.* **92**, 1343 (2003).
9. G. Gaucher, M. H. Dufresne, V. P. Sant, N. Kang, D. Maysinger and J. C. Leroux, *J. Control. Rel.* **109**, 169 (2005).
10. R. G. Schoenmakers, P. van de Wetering, D. L. Elbert and J. A. Hubbell, *J. Control. Rel.* **95**, 291 (2004).
11. Z. Xie, H. Guan, X. Chen, C. Lu, L. Chen, X. Hu, Q. Shi and X. Jing, *J. Control. Rel.* **117**, 210 (2007).
12. K. Ulbrich and V. Subr, *Adv. Drug Deliv. Rev.* **56**, 1023 (2004).
13. E. R. Gillies, A. P. Goodwin and J. M. J. Frechet, *Bioconjug. Chem.* **15**, 1254 (2004).
14. V. S. Trubetskoy and V. P. Torchilin, *Adv. Drug Deliv. Rev.* **16**, 311 (1995).
15. N. Nishiyama and K. Kataoka, *Curr. State Pharmacol. Ther.* **112**, 630 (2006).
16. D. Kim, Z. G. Gao, E. S. Lee and Y. H. Bae, *Mol. Pharm.* **6**, 1353 (2009).
17. Y. Bae, N. Nishiyama and K. Kataoka, *Bioconjug. Chem.* **18**, 1131 (2007).
18. M. Sirova, J. Strohalm, V. Subr, D. Plocova, P. Rossmann, T. Mrkvan, K. Ulbrich and B. Rihova, *Cancer Immunol. Immunother.* **56**, 35 (2007).
19. J. W. Hopewell, R. Duncan, D. Wilding and K. Chakrabarti, *Human Exp. Toxicol.* **20**, 461 (2001).
20. H. S. Yoo and T. G. Park, *J. Control. Rel.* **96**, 273 (2004).
21. K. Ulbrich, T. Etrych, P. Chytil, M. Jelinkova and B. Rihova, *J. Drug Target.* **12**, 477 (2004).
22. Y. J. Lu and P. S. Low, *Adv. Drug Deliv. Rev.* **54**, 675 (2002).
23. J. Sudimack and R. J. Lee, *Adv. Drug Deliv. Rev.* **41**, 147 (2000).
24. C. Deng, X. Chen, H. Yu, J. Sun, T. Lu and X. Jing, *Polymer* **48**, 139 (2007).
25. C. Deng, G. Rong, H. Tian, Z. Tang, X. Chen and X. Jing, *Polymer* **46**, 653 (2005).
26. C. Deng, H. Tian, P. Zhang, J. Sun, X. Chen and X. Jing, *Biomacromolecules* **7**, 590 (2006).

27. T. Lu, J. Sun, X. Chen, P. Zhang and X. Jing, *Macromol. Biosci.* **9**, 1059 (2009).
28. Z. Xie, X. Hu, X. Chen, T. Lu, S. Liu and X. Jing, *J. Appl. Polym. Sci.* **110**, 2961 (2008).
29. Z. Xie, T. Lu, X. Chen, C. Lu, Y. Zheng and X. Jing, *J. Appl. Polym. Sci.* **105**, 2271 (2007).
30. X. Zhang, Y. Li, X. Chen, X. Wang, X. Xu, Q. Liang, J. Hu and X. Jing, *Biomaterials* **26**, 2121 (2005).
31. X. Hu, S. Liu, X. Chen, G. Mo, Z. Xie and X. Jing, *Biomacromolecules* **9**, 553 (2008).
32. Z. Xie, H. Guan, L. Chen, H. Tian, X. Chen and X. Jing, *Polymer* **46**, 10523 (2005).
33. H. F. Liu, W. W. Liu and D. C. Fang, *World Chin. J. Digestol.* **8**, 1361 (2000).
34. A. Y. Chang, J. Rubins, R. Asbury, L. Boros and L. F. Hui, *Semin. Oncol.* **28**, 10 (2001).
35. R. T. Allen, W. J. Hunter and D. K. Agrawal, *J. Pharmacol. Toxicol. Methods* **37**, 215 (1997).
36. J. P. Aubry, H. Blaecke, S. Lecoanet-Henchoz, P. Jeannin, N. Herbault, G. Caron, V. Moine and J. Y. Bonnefoy, *Cytometry* **37**, 197 (1999).